Research Article

Joseph Tsemeugne*, Pamela Kemda Nangmo, Pierre Mkounga, Jean De Dieu Tamokou, Iréne Chinda Kengne, Giles Edwards, Emmanuel Fondjo Sopbué and Augustin Ephrem Nkengfack

Synthesis, characteristic fragmentation patterns, and antibacterial activity of new azo compounds from the coupling reaction of diazobenzothiazole ions and acetaminophen

https://doi.org/10.1515/hc-2020-0127
received April 08, 2021; accepted August 18, 2021

Abstract: In this study, a series of azobenzothiazole dyes **4** were synthesized via diazotization of substituted benzothiazole derivatives followed by azo coupling with acetaminophen. The chemical structures of all synthesized compounds were confirmed using analytical data and spectroscopic techniques, including UV-visible, IR, mass spectra, and ^{1}H- and ^{13}C-NMR. The in situ formed diazobenzothiazole ions regiospecifically react with acetaminophen derivatives in the Hollemann-guided electrophilic aromatic substitution mechanism. The regio-orientations were established, on the one hand, by a rigorous interpretation of ^{1}H-NMR spectra and, on the other hand, by the characteristic fragmentation patterns observed on the electrospray mass spectra. In the cases of **4a** and **4b,** multisubstitutions occurred. The antimicrobial activity of compound **4**, along with all the starting materials, was investigated on *Pseudomonas aeruginosa* PA01, *Staphylococcus aureus* 18, *Escherichia coli* 64R, and *S. aureus* ATCC 25923. The results showed that this skeletal framework exhibited marked potency as antibacterial agents. The most active antibacterial agent against both targeted organisms was compound **4a′**.

Keywords: benzothiazole, acetaminophen, azo dyes, fragmentations, antibacterial studies

*** Corresponding author: Joseph Tsemeugne,** Laboratory of Natural Products and Applied Organic Synthesis (LANAPOS), Department of Organic Chemistry, University of Yaounde I, P.O. Box 812, Yaounde, Republic of Cameroon, e-mail: tsemeugne@yahoo.fr
Pamela Kemda Nangmo: Laboratory of Natural Products and Applied Organic Synthesis (LANAPOS), Department of Organic Chemistry, University of Yaounde I, P.O. Box 812, Yaounde, Republic of Cameroon; Institute of Medical Research and Medicinal Plants Studies (IMPM), Ministry of Scientific Research and Innovation, P.O. Box 13033, Yaounde, Republic of Cameroon
Pierre Mkounga, Augustin Ephrem Nkengfack: Laboratory of Natural Products and Applied Organic Synthesis (LANAPOS), Department of Organic Chemistry, University of Yaounde I, P.O. Box 812, Yaounde, Republic of Cameroon
Jean De Dieu Tamokou, Iréne Chinda Kengne: Laboratory of Microbiology and Antimicrobial Substances, Department of Biochemistry, Faculty of Science, University of Dschang, P.O. Box 067, Dschang, Republic of Cameroon
Giles Edwards: Department of Physics and Astronomy, The University of Manchester, Oxford Road, Manchester, M13 9PL, Oxford, United Kingdom
Emmanuel Fondjo Sopbué: Laboratory of Applied Synthetic Organic Chemistry, Department of Chemistry, Faculty of Science, University of Dschang, P.O. Box 67, Dschang, Republic of Cameroon

1 Introduction

In most of our societies, pain and discomfort are often treated with analgesics drugs [1]. Analgesics are also widely used to treat dysphoric moods and sleep disturbances [2]. It is now established that there is a link between rates of the use of pain relievers and certain psychiatric illnesses such as depressive symptoms, alcohol, nicotine, and caffeine consumption [3]. However, the most common side effects associated with the consumption of analgesic drugs are gastrointestinal disorders [4]. Inhibition of prostaglandin formation in the stomach by most pain-relieving drugs can lead to inflammation, injury, and a stomach ulcer [5]. One of the advantages of acetaminophen is that it does not cause gastrointestinal problems like most other nonsteroidal anti-inflammatory drugs [1,6], and this is due to acetaminophen's low affinity for cyclooxygenase (COX). However, like most drugs, acetaminophen has several side effects, the most important of which is liver damage, often even at therapeutic doses [7,8]. Acetaminophen, a nonsteroidal anti-inflammatory

drug, could follow some transformations like binding it to the benzothiazole ring to improve its nephrotoxicity. Benzothiazoles are aromatic heterocycles known for their anti-inflammatory [9–11], antibacterial [12], antifungal [13], antiviral [14], and antidiabetic [15] activities. To continue our search to find a better combination of pharmacophores within diazo molecules for pharmaceutical applications [16–20], we prepared a series of diazobenzothiazole ions, which were copulated with acetaminophen.

2 Results and discussion

2.1 Chemistry

The synthetic strategies adopted for the synthesis of the target compounds are depicted in Scheme 1. The structures of **4** were established based on their elemental analyses and spectral data.

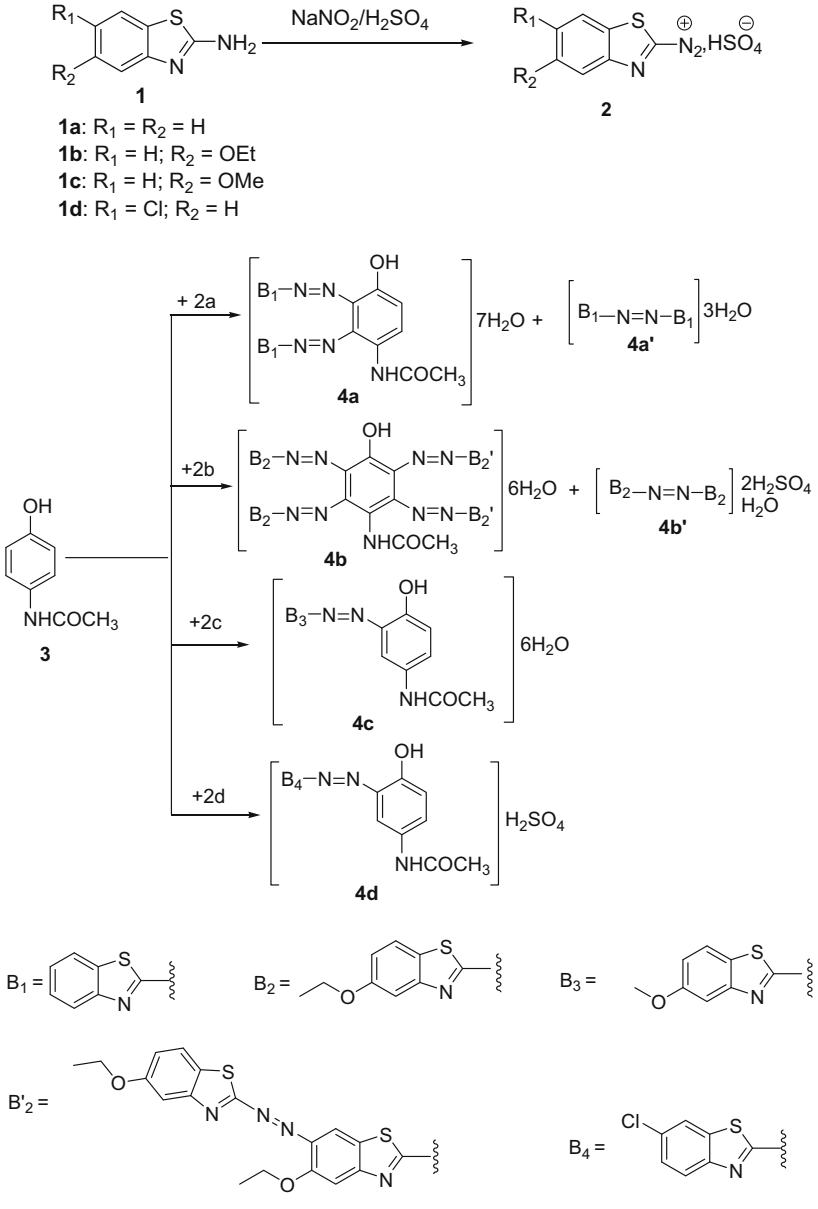

Scheme 1: Sequence of reactions leading to compounds **4** synthesis.

Diazotisation of 2-aminobenzothiazole **1** in strong acids yields diazonium salts **2,** which undergo coupling reactions with acetaminophen **3** (Scheme 1).

The electronic transition of UV-visible spectra in methanol gave rise to wavelength (λ_{max}) ranging from 272 to 515 nm. The first wavelength (λ_{max}) for all the compounds was found between 272 and 276 nm as a result of $\pi \rightarrow \pi^*$ transition of the compounds, indicating the presence of C=C atypical to benzene nucleus. The other wavelength of the benzenoid region (i.e., between 436 and 486 nm) was dole out as a result of $n \rightarrow \pi^*$ transition and extended conjugation contributed by the C=C and the conjugative linkage performed by the N=N group. An incomparably strong bathochromic shift occurred in compound **4d** that resulted in the wavelength at far visible region of light at λ_{max} of 515 nm ($\log \varepsilon = 3.26$) was due to the presence of an auxochrome (–Cl) in the skeletal framework of compound **4d,** which improved the color deepening attribute by delocalization of the lone pair of electron present on the chlorine atom [21,22].

The infrared spectra of synthesized dyes **4** showed between 3,300 and 3,200 cm^{-1} a complex broad absorption band that may be assigned to the combined stretching bands of the phenolic O–H group and H_2O molecule. The infrared spectra of compounds **4** also showed absorption bands due to the stretching vibrations of C=C of aromatic and Ar C–H bending vibration at 1,599–1,525 cm^{-1} and 889–631 cm^{-1}, respectively. The FT-IR spectra also showed a band at 1,496–1,405 cm^{-1} assigned to the N=N group of the azo dyes and a band at 1,260–1,256 cm^{-1} assigned to the C–S of benzothiazole molecule [23].

The reaction of the diazonium salt solution **2a** with **3** gave the two coupling products: **4a** and **4a′** (Scheme 1). Compound **4a** was obtained as brown powder melting between 262 and 264°C and crystallizing with seven H_2O molecules. The presence of two characteristic doublets at $\delta_H = 7.11$ (d, $J = 8.8$ Hz, H-5′) and $\delta_H = 7.49$ (d, $J = 8.8$ Hz, H-6′) on the ^{1}H-NMR spectrum of compound **4a** suggests that the coupling reaction took place at the 2′ and 3′ position of paracetamol ring system in agreement with recent findings [16]. On the ^{1}H-NMR spectrum, besides the set of five multiplets appearing between 8.49 and 7.03 ppm attributable to the ten aromatic protons, two broad D_2O-exchangeable signals were observed around 10.00 and 2.50 ppm and assigned to the H_2O and OH protons, respectively.

Further supporting evidences were obtained from the elemental analysis and the electrospray mass spectra, which confirmed the molecular mass to be 599, with relevant ion fragments at $m/z = 598$ ($M^{+\cdot} - H$), 581 ($M^{+\cdot} - H_2O$), 565 ($M^{+\cdot} - H_2O - CH_4$), 539 ($M^{+\cdot} - CH_3CONH_2 - H$), 508 ($M^{+\cdot} - H - 5H_2O$), 507 ($M^{+\cdot} - 2H_2O - 2N_2$), 465 ($M^{+\cdot} - C_7H_5NS$), and 313 ($M^{+\cdot} - H_2O - 2C_7H_4NS$). The ion fragment at $m/z = 479$ ($M^{+\cdot} - 2N_2 - 2S$), 461 ($M^{+\cdot} - 2N_2 - 2S - H_2O$), 404 ($M^{+\cdot} - 2N_2 - 2S - H_2O - CH_3CON$), and 327 ($M^{+\cdot} - 2N_2 - 2S - 2C_6H_4$) was assigned as in Scheme 2, confirming the aforementioned structural hypothesis.

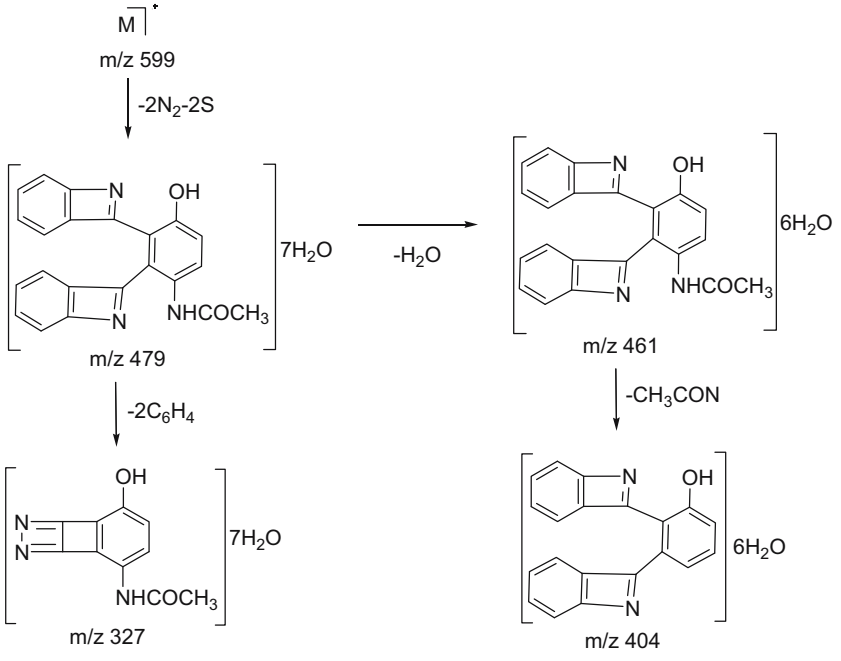

Scheme 2: Significant HRESI-MS fragmentation patterns of compound **4a**.

The azo-structures **4a′,** which was a byproduct from the reaction of diazobenzothiazole **1a** with acetaminophen, was reported earlier by other authors (but without water crystallites) resulting from the oxidation of 2-aminobenzothiazole **1a** by sodium hypochlorite [24,25]. Compound **4a′** was obtained as a dark red powder; its elemental analysis and HREIMS experiments enabled us to establish its gross formula to be $C_{14}H_{14}N_4O_3S_2$, showing that the coupling product crystallized with three molecules of H_2O. These results agreed with the IR experiment, which exhibited a large band in the higher frequency region around 3,273 cm^{-1} due to the hydroxyl groups of H_2O.

The electrospray mass spectra showed the molecular ion peak at m/z 350 corresponding to ($M^{+\cdot}$ – H). The following characteristic ion fragments were rationalized as follows at m/z = 335 ($M^{+\cdot}$ – NH), 316 ($M^{+\cdot}$ – H_2S), 299 ($M^{+\cdot}$ – H_2O – HS), 273 ($M^{+\cdot}$ – H – C_6H_4), and 204 ($M^{+\cdot}$ – $3H_2O$ – N_2 –2S). The ion fragments at m/z = 215 ($M^{+\cdot}$ – NH_3 – C_7H_2S), 159 ($M^{+\cdot}$ – NH_3 – $3H_2O$ – C_7H_4S), and 86 ($M^{+\cdot}$ – NH_3 – $3H_2O$ – $C_{13}H_5S$) were assigned as in Scheme 3, confirming the aforementioned structural hypothesis.

We also studied the surface H_2O exchange behaviors of compounds **4a′** by primary alcohols using electrospray ionization mass spectrometry (ESI-MS) [26,27]. Methanol was used as a model primary alcohol for the analysis. As clearly proven by peaks at m/z = 328, 300, 176, and 148

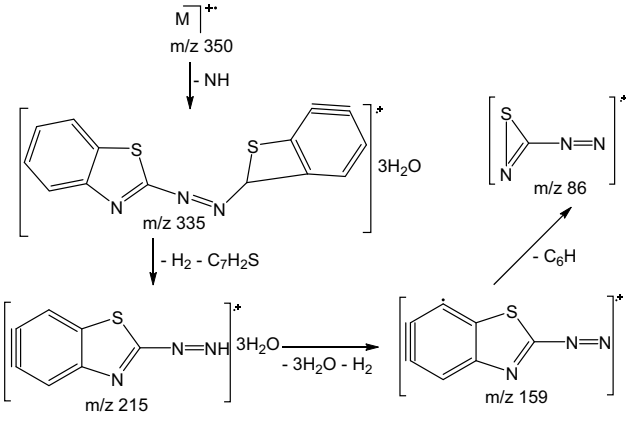

Scheme 3: Significant HRESI-MS fragmentation patterns of compound **4a′**.

surface of azobenzothiazole dye **4a′** is fully exchanged by methanol within 1 min to give various peaks ($M^{+\cdot}$ – $3H_2O$ + MeOH), ($M^{+\cdot}$ – $3H_2O$ – N_2 + ′MeOH), ($M^{+\cdot}$ – $3H_2O$ – $2C_6H_4$ + MeOH), and ($M^{+\cdot}$ – $3H_2O$ – $2C_6H_4$ – N_2 + MeOH), respectively.

The ^{1}H-NMR spectrum of compound **4a′** exhibits in the range 8.15–7.55 ppm a series of signals corresponding to the eight aromatic protons. The ^{13}C (^{1}H)-NMR experiment exhibited exactly seven signals, among which a downfield signal at 198.6 ppm is assigned to C-2 and C-2′ carbon of benzothiazole.

The reaction of diazotized **2b** with **3** gave the coupling products **4b** and **4b′** (Scheme 1). It should be pointed out that compound **4b′** was formed in the same manner as compound **4a′**. This compound resulting from the *in situ* deaminated [28,29] intermediate product **2b′** probably underwent coupling with the diazobenzothiazole ion **2b** to yield compound **4b′** (Scheme 4).

Compound **4b′** was obtained as brown powder with a melting point of 182–184°C. The elemental analysis and the electrospray mass spectra experiments were used to establish the gross formula as $C_{18}H_{22}N_4O_{11}S_4$, showing that the coupling product crystallized with two molecules of H_2SO_4 and one molecule of H_2O. These results were confirmed by the IR experiment, which exhibited a large band in the higher frequency region around 3,275 cm^{-1}, resulting from the combined stretching frequencies of the hydroxyl groups of H_2SO_4 and H_2O.

The HRESI-MS showed the molecular ion (M^+ + H) peak at m/z 599. The following characteristic ion fragments were rationalized as follows at m/z = 583 ($M^{+\cdot}$ – CH_3), 569 ($M^{+\cdot}$ – CH_3CH_2), 549 ($M^{+\cdot}$ + H – H_2O – S), 535 ($M^{+\cdot}$ – H_2O – C_2H_5O), 410 ($M^{+\cdot}$ – H_2SO_4 – $2C_2H_5O$), 400 ($M^{+\cdot}$ – $2H_2SO_4$ – H_2), 357 (M^+ + H$^\cdot$ – H_2O – $2H_2SO_4$ – N_2), and 283 ($M^{+\cdot}$ + H – $2H_2SO_4$ – C_8H_8O).

The ^{1}H-NMR spectrum of compound **4b′** shows two signals at δ 1.23 and 4.13, and three multiplets at δ 8.01, 7.91, and δ 7.09, respectively, attributable to the protons CH_3 and CH_2 of the ethoxy group and protons' sets (H-4 and H-4′), (H-7 and H-7′), and (H-5 and H-5′) of the benzothiazole.

Compound **4b** was obtained as red powder melting at 197–199°C and crystallizing with six H_2O molecules. Further supporting evidence was obtained from the

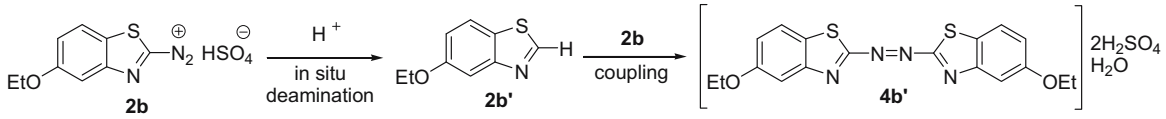

Scheme 4: Reaction sequence to compounds **4b′**.

elemental analysis and the HREIMS, which confirmed the molecular mass to be 1,490, with relevant ion fragments at m/z = 1,453 ($M^{+\cdot} - H - 2H_2O$), 1,428 ($M^{+\cdot} - HO - C_2H_5O$), 1,404 ($M^{+\cdot} - 3H_2O - S$), 1,379 ($M^{+\cdot} - 3H_2O - CH_3CON$), 1,353 ($M^{+} - H^{\cdot} - 6H_2O - N_2$), 1,323 ($M^{+\cdot} - 6H_2O - CH_3CONH_2$), 1,293 ($M^{+\cdot} - HO - 4C_2H_5O$), and 1,238 ($M^{+\cdot} - 4H_2O - 4C_2H_5O$).

The ^{13}C-NMR spectrum of compound **4b** exhibited 59 carbon signals instead of 62 as required by the molecular formula. That could be explained by overlapping the signals of three methyl substituents of the ethoxy group at δ_C 19.9 ppm and carbon C-2″ and C-2^{vi} at δ_C 178.3 ppm due to their magnetic and chemical equivalence. The assignment of ^{1}H- and ^{13}C(^{1}H)-NMR data for compound **4b** was done by comparison with the simulated values (Table 1).

Based on the comparison of the full width at half maximum (FWHM) of protons H-7, H-7^{vi}, H-7, and H-7 of compounds **4a**, **4b**, **4c**, and **4d** (1.80 kHz for **4a**, 0.99 kHz for **4b**, 1.31 kHz for **4c**, and 0.50 kHz for **4d**), respectively, it could be concluded that there is a stronger π–π stacking interaction between molecules in **4a** sample than in **4c**, **4b**, and **4d** samples. Stronger π–π stacking interaction between molecules will lead to stronger ^{1}H–^{1}H dipolar couplings as well as the increase of anisotropic bulk magnetic susceptibility (ABMS), both of which will lead to the broadening of aromatic proton peaks [30].

We also calculated the values of the full width at half maximum (FWHM) of protons H-7 for compounds **4a′** and **4b′**. The full width at half maximum of **4a′**, which is of the order of 0.89 kHz, is greater than that of **4b′**, which is of the order of 0.50 kHz.

The structures of compounds **4c** and **4d** were assigned based on their analytical and spectral data by following similar reasoning as earlier.

3 Antimicrobial activity

Benzothiazole **1,** acetaminophen **3**, and azo products **4** exhibited different degrees of antibacterial activities against the tested bacteria (Table 2).

Compounds **1d** and **3** did not show any antibacterial activity on all the tested microorganisms. Compounds **1a** and **1c** were active only against *Pseudomonas aeruginosa* PA01. Optimization of compound **1a** by substitution of the benzene part of the benzothiazole ring at position 5 with a hydrophobic group (5-ethoxy-) resulted in improved antibacterial activities of compound **1b** against *P. aeruginosa*, *E. coli*, and *S. aureus* compared with the 5-methoxy group (compound **1c**) or to unsubstituted benzothiazole (compound **1a**). Similar to our finding, a previous study has demonstrated that derivatives with 5-chloro, 5-propyl, 5-ethoxy, 5-bromo, and 5-trifluoromethyl groups at position 5 of the benzothiazole ring improved antibacterial activities against *S. aureus*, while the polar 5-OH substituent showed drastically decreased activity [31]. Benzothiazole **1b** and reaction product **4** displayed antibacterial activities against all the tested bacteria. The antibacterial activities of reaction products are sometimes equal to or greater than those of ciprofloxacin used as a reference antibiotic. Overall, compound **4a′** was the most active, followed in a decreasing order by compounds **4b**, **4a**, **4c**, **4d**, **4b′,** and **1b**. Differences in the antibacterial activities of compounds **4** may be due to the nature of the substituents on the phenyl ring of the benzothiazole backbone. The lowest MIC value (4 μg/mL) corresponding to the greatest antibacterial activity was obtained with compound **4a′** against *P. aeruginosa* PA01 and *Staphylococcus aureus* ATCC 25923, while the lowest value of MBC (32 μg/mL) was recorded with compound **4a′** against *P. aeruginosa* PA01 and *S. aureus* ATCC 25923 as well as with compound **4b** against *P. aeruginosa* PA01. The highest MBC value (128 μg/mL) was recorded with **4a** and **4b** against *S. aureus* 18 and *Escherichia coli* 64 R and with **4a′** on *S. aureus* 18. *S. aureus* 18 and *E. coli* 64 R were the most resistant bacteria, whereas *P. aeruginosa* PA01 and *S. aureus* ATCC 25923 were the most sensitive organisms. Compounds **1b**, **4c**, **4d**, **4a′**, and **4b′** (MBC/CMI >4) showed bacteriostatic activities on the sensitive bacteria, while compounds **4a** and **4b** showed bactericidal effects on all the tested bacteria. Several benzothiazole-based compounds have shown promising activities against several Gram-positive and Gram-negative bacteria and also against *Mycobacterium tuberculosis* [31]. It was found that their modes of antibacterial action are due to the inhibition of enzymes that are important for essential processes in the bacterial cells, such as cell wall synthesis, cell division, and DNA replication, or are important for different biosynthetic pathways of essential compounds in bacterial cells, such as the biosynthesis of histidine and biotin [32]. Therefore, we assume that the modes of antibacterial action of our compounds might be similar to those of analogous compounds already described in the literature.

4 Conclusion

This investigation proposes a useful method for the synthesis of heterocyclic azo dyes incorporating moieties of acetaminophen, which is an analgesic pharmacophore. Compounds **4** exhibited good antibacterial activity against all bacterial strains due to the presence of benzothiazole

Table 1: Comparison of ^{1}H- and $^{13}C(^{1}H)$-NMR data of 4b with the simulated values

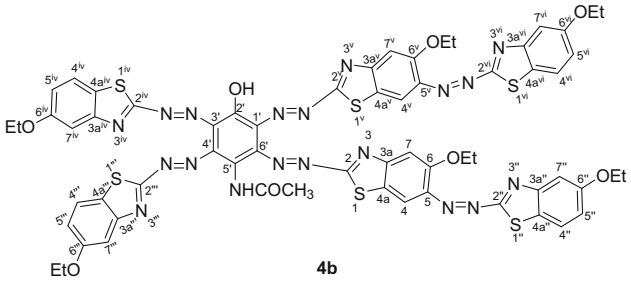

4b

	δ_H in ppm (multiplicity, *J* in Hz)		δ_C in ppm	
N° (H, C)	**Simulated values**	**Experimental values**	**Simulated values**	**Experimental values**
2, 2″, 2‴, 2^{iv}, 2^{v}, 2^{vi}			166.4; 166.4; 160.4; 160.4; 160.4; 160.4	178.3; 178.3; 174.5; 173.7; 173.4; 173.2
3a, 3a″, 3a‴, $3a^{iv}$, $3a^{v}$, $3a^{vi}$			151.1; 151.1; 151.1; 151.1; 150.9; 150.9	152.0; 152.0; 151.0; 150.1; 157.2; 156.9
4a, 4a″, 4a‴, $4a^{iv}$, $4a^{v}$, $4a^{vi}$			136.5; 136.1; 131.8; 131.8; 131.8; 131.8;	137.4; 137.3; 130.4; 128.7; 128.0; 127.8
4, 4″, 4‴, 4^{iv}, 4^{v}, 4^{vi}	8.36 (d, 1H, *J* = 0.4, H-4), 7.50 (dd, 1H, *J* = 7.8 and 0.4, H-4″), 7.53 (dd, 1H, *J* = 7.7 and 0.4, H-4‴), 7.51 (dd, 1H, *J* = 7.8 and 0.4, H-4^{iv}), 8.34 (d, 1H, *J* = 0.4, H-4^{v}), 7.49 (dd, 1H, *J* = 7.8 and 0.4, H-4^{vi}),	7.58 (s, 1H, H-4), 7.65 (d, 2H, *J* = 8.8, H-4″ and H-4^{vi}), 7.91 (d, 1H, *J* = 9.2, H-4‴), 8.11 (d, 1H, *J* = 2.8, H-4^{iv}), 7.61 (s, 1H, H-4^{v})	110.0; 110.0; 105.5; 105.5; 105.5; 105.5;	111.7; 111.4; 110.8; 110.2; 105.9; 109.9
5, 5″, 5‴, 5^{iv}, 5^{v}, 5^{vi}	6.99 (dd, 1H, *J* = 7.8 and 1.4, H-5″), 7.15 (dd, 1H, *J* = 7.7 and 1.4, H-5‴), 7.12 (dd, 1H, *J* = 7.8 and 1.4, H-5^{iv}), 6.98 (dd, 1H, *J* = 7.8 and 1.4, H-5^{vi})	7.09 (dd, 2H, *J* = 8.8, H-5″ and H-5^{vi}), 7.16 (dd, 2H, *J* = 9.2 and 2.8, H-5‴ and H-5^{iv})	155.8; 155.8; 155.8; 155.8; 145.8; 145.8	163.6; 163.3; 161.8; 161.7; 161.4; 158.5
6, 6″, 6‴, 6^{iv}, 6^{v}, 6^{vi}			115.5; 115.5; 115.5; 115.5; 133.6; 133.6	122.1; 121.7; 121.4; 123.5; 141.1; 140.9
7, 7″, 7‴, 7^{iv}, 7^{v}, 7^{vi}	7.43 (d, 1H, *J* = 0.4, H-7), 7.37 (dd, 1H, *J* = 1.4 and 0.4, H-7″), 7.55 (dd, 1H, *J* = 1.4 and 0.4, H-7‴), 7.52 (dd, 1H, *J* = 1.4 and 0.4, H-7^{iv}), 7.38 (d, 1H, *J* = 0.4, H-7^{v}), 7.36 (dd, 1H, *J* = 1.4 and 0.4, H-7^{vi})	8.00 (s, 1H, H-7), 7.68 (d, 1H, *J* = 3.6, H-7″), 7.71 (d, 1H, *J* = 2, H-7‴), 7.15 (d, 1H, *J* = 2.4, H-7^{iv}), 8.02 (s, 1H, H-7^{v}), 7.62 (d, 1H, *J* = 6.4, H-7^{vi})	124.3; 124.3; 103.4; 103.4; 118.1; 118.1	123.9; 123.8; 120.9; 120.7; 117.2; 113.4
1′			130.7	133.1
2′			147.9	143.6
3′			140.5	141.8
4′			140.5	141.5
5′			135.5	136.9
6′			130.7	130.4
CO			168.7	199.1
CH_3CO	2.15 (s, 3H)	2.52 (s, 3H)	24.0	29.0
OCH_2CH_3	4.49; 4.47; 4.34; 4.30; 4.54; 4.62	4.18; 4.16; 4.14; 4.12; 4.11; 4.10	63.7	74.9; 71.1; 70.7; 69.1; 69.0; 68.9
OCH_2CH_3	1.29; 1.29; 1.29; 1.29; 1.32; 1.31	1.58; 1.40; 1.38; 1.36; 1.35	14.7	20.0; 19.9; 19.8; 19.7
NH		10.66		
OH		3.27		

Table 2: Antimicrobial activity (MIC and MMC in μg/mL) of synthesized compounds as well as reference antimicrobial drugs

Compounds	Inhibition parameters	*Pseudomonas aeruginosa* PA01	*Staphylococcus aureus* 18	*Escherichia coli* 64R	*Staphylococcus aureus* ATCC 25923
1a	MIC	128	>256	>256	>256
	MMC	>256	—	—	—
	MMC/MIC	—	—	—	—
1b	MIC	64	128	64	64
	MMC	>256	>256	>256	>256
	MMC/MIC	—	—	—	—
1c	MIC	128	>256	>256	>256
	MMC	>256	—	—	—
	MMC/MIC	—	—	—	—
1d	MIC	>256	>256	>256	>256
	MMC	—	—	—	—
	MMC/MIC	—	—	—	—
3	MIC	>256	>256	>256	>256
	MMC	—	—	—	—
	MMC/MIC	—	—	—	—
4a	MIC	16	32	32	16
	MMC	64	128	128	64
	MMC/MIC	4	4	4	4
4b	MIC	8	64	32	16
	MMC	32	128	128	64
	MMC/MIC	4	2	4	4
4c	MIC	8	64	32	32
	MMC	64	>256	>256	>256
	MMC/MIC	8	—	—	—
4d	MIC	16	64	32	32
	MMC	>256	>256	>256	>256
	MMC/MIC	—	—	—	—
4a′	MIC	4	16	8	4
	MMC	32	128	64	32
	MMC/MIC	8	8	8	8
4b′	MIC	16	64	32	32
	MMC	>256	>256	>256	>256
	MMC/MIC	—	—	—	—
Ciprofloxacin	MIC	32	16	16	8
	MMC	64	32	16	8
	MMC/MIC	2	2	1	1

—: not determined; MIC: minimum inhibitory concentration; MBC: minimum bactericidal concentration.

backbone and N=N group in the same molecular structural frame. A more extensive study is needed to confirm the preliminary results and to assess anti-inflammatory activity of this series of compounds.

5 Experimental

5.1 General information

Melting points were determined on a Buchii melting point apparatus. The thin layer chromatography (TLCs) was carried out on Eastman Chromatogram Silica Gel Sheets (13,181; 6,060) with fluorescent indicators. A mixture of hexane and ethyl acetate (4:6) was used as the eluent and iodine was used for the visualization of the chromatograms. The IR spectra were measured with a Fourier transform infrared spectrometer JASCO FT/IR-4100 and a Perkin Elmer FT-IR 2000 spectrometer. The UV spectra were recorded with a Beckman U-640 Spectrophotometer using samples' solutions of concentration 5×10^{-5} mol/L. Combustion analyses were carried out with a Euro EA CHNSO analyzer from Hekatech Company, and the results were found to be in good agreement (±0.3%) with the calculated values. Positive ion electrospray mass spectra were recorded on a Waters Xevo TQD tandem quadrupole mass spectrometry system running in an MS scan mode, and 1 min of acquired spectra was combined and

centroided. ^{1}H-NMR spectra were recorded in DMSO-d_6 with a 400 MHz spectrometer RMN Bruker Advance 400. ^{13}C-NMR spectra were recorded in DMSO-d_6 with a 100 MHz spectrometer RMN Bruker Advance 400. Tetramethylsilane (TMS) was used as the internal reference. Simulated ^{1}H- and ^{13}C(^{1}H)-NMR-spectra were performed using http://www.nmrdb.org/spectral simulation software.

5.2 Preparation of the reagents and starting materials

All the reagents mentioned in this study were purchased from Aldrich and Fluka and were used without further purification.

5.3 Preparation of diazonium salt solution

In a similar manner as described earlier [20], dried sodium nitrite (0.69 g, 10 mmol) was slowly added over a period of 30 min to concentrated sulfuric acid (10 mL) with occasional stirring. The solution was cooled to 0–5°C. Compound **1** was dissolved in DMSO (10 mL) and cooled to 0–5°C. The nitrosyl sulfuric acid solution was added to the solution of **1**, and the temperature was maintained between 0 and 5°C. The clear diazonium salt solution thus obtained consisting of the *in situ*-formed intermediate **2** was used immediately in the coupling reactions.

5.4 General procedure for the preparation of the coupling products 4a–d

Acetaminophen (1.51 g, 10 mmol) **3** was dissolved in DMSO (10 mL) and then cooled in an ice bath at 0–5°C. The previously prepared diazonium solution of **2** was added dropwise over 1 h, and then 15 mL of sodium acetate solution (10%) was added to the mixture. The pH of the mixtures ranged from 9 to 11. The solid precipitate was collected on a filter and crystallized from methanol to give the title compound.

5.4.1 *N*-(3-(Benzo[*d*]thiazol-2-yldiazenyl)-2-(benzo[*d*]thiazol-2-yldiazenyl)-4-hydroxyphenyl) acetamide heptahydrate (4a)

Compound **4a** was obtained in 31% yield as brown powder; m.p. 262–264°C (dec); ^{1}H-NMR (DMSO-d_6, 400 MHz): δ 8.45 (d, 1H, J = 2.4, H-7″), 8.14 (dd, 1H, J = 2.8 and 8.4, H-7), 8.05 (d, 1H, J = 8.4, H-4), 7.68 (ddd, 1H, J = 2.4, 6.8 and 9.2, H-5″), 7.65 (ddd, 1H, J = 2.4, 6.4 and 8.8, H-5), 7.61 (d, 1H, J = 7.6, H-6), 7.58 (ddd, 1H, J = 8.0, 6.4 and 1.6, H-6″), 7.54 (dd, 1H, J = 8.4 and 1.2, H-4″), 7.49 (d, 1H, J = 8.8, H-6'), 7.11 (d, 1H, J = 8.8, H-5'), 2.5 (s, 3H, $COCH_3$); ^{13}C-NMR (DMSO-d_6, 100 MHz): δ 175.5 (CO), 168.1 (C-2 and C-2′), 153.9 (C-4′), 152.2 (C-3a and C-3a″), 138.4 (C-2′ and C-3′), 133.8 (C-4a and C-4a″), 132.1 (C-1′), 128.6 (C-6), 127.4 (C-6″), 126.9 (C-5 and C-5″), 124.2 (C-4 and C-4″), 122.9 (C-7″), 122.0 (C-7), 118.9 (C-6′), 107.8 (C-5′), 23.8 (CH_3); UV-Vis λ_{max} (DMSO) (log ε): 221 (3.82), 267 (4.05), 322 (4.03), 340 (4.05), 376 (4.06), 384 (4.05), 413(3.98), 428 (3.94), 442 (3.91), 507 (3.68) nm; IR (KBr) ν_{max}: 3,269 (O–H), 2,916–2,847 (Ar C–H), 1,663 (C=O), 1,528 (C=C), 1,496–1,433 (N=N), 1,312 (C–S), 1,239 (C–O), 881–645 (Ar def C=N str thiazole) cm^{-1}; ms: (ESI^{+}) m/z (%) 581 (2), 508 (2), 507 (14), 447(80), 449 (53), 342 (75), 309 (82), 281 (75), 147 (45), 133 (100), 98 (3); anal. calcd for $C_{22}H_{27}N_7O_8S_2$: C, 45.43; H, 4.68; N, 16.86; S, 11.02. Found: C, 45.39; H, 4.68; N, 16.87; S, 11.03. Rf = 0.54.

5.4.2 1,2-Bis(benzo[*d*]thiazol-2-yl)diazene trihydrate (4a′)

Compound **4a′** was obtained in 11% as dark red powder; m.p. ≥360°C (dec) {Lit. m.p. 295°C, [24]}; ^{1}H-NMR (DMSO-d_6, 400 MHz): δ 8.15 (d, 2H, J = 2.4, H-7 and H-7′), 7.62 (ddd, 2H, J = 8.8, 7.8 and 1.6, H-4 and H-4′), 7.55 (ddd, 2H, J = 7.8, 8.8 and 1.6, H-6 and H-6′), 7.66 (d, 2H, J = 2.4, H-5 and H-5′); ^{13}C-NMR (DMSO-d_6, 100 MHz): δ 198.6 (C-2 and C-2′), 153.9 (C-4a and C-**4a′**), 132.1 (C-3a and C-3a′), 124.5 (C-5 and C-5'), 120.7 (C-6 and C-6′), 118.9 (C-7 and C-7′); 105.4 (C-4 and C-4′); UV-Vis λ_{max} (DMSO) (log ε): 219 (3.83), 229 (3.82), 266 (4.01), 284 (3.97), 315 (4.02), 321 (4.02), 344 (4.07), 356 (4.09), 467 (3.78), 492 (3.72) nm; IR (KBr) ν_{max}: 3,273 (O–H), 1,661 (C=N), 1,532 (C=C), 1,498–1,419 (N=N), 888–610 (Ar def C=N str thiazole) cm^{-1}; ms: (ESI^{+}) m/z (%) 349 (8), 335 (3), 291 (13), 299 (6), 233 (34), 175 (41), 116 (61), 73 (74), 57 (100); anal. calcd for $C_{14}H_{14}N_4O_3S_2$: C, 47.99; H, 4.03; N, 15.99; S, 18.30. Found: C, 47.97; H, 3.99; N, 15.97; S, 18.32. Rf = 0.69.

5.4.3 *N*-(2-(6-Ethoxy-5-((6-ethoxybenzo[*d*]thiazol-2-yl)diazenyl)benzo[*d*]thiazol-2-yl)diazenyl)-3-((6-ethoxy-5-((6-ethoxybenzo[*d*]thiazol-2-yl)diazenyl)benzo[*d*]thiazol-2-yl)diazenyl)-5,6-bis((6-ethoxybenzo[*d*]thiazol-2-yl)diazenyl)-4-hydroxyphenyl)acetamide hexahydrate (4b)

Compound **4b** was obtained in 47% yield as red powder; m.p. 197–199°C (dec); ^{1}H-NMR (DMSO-d_6, 400 MHz): δ

8.11 (d, 1H, J = 2.8, H-4^{iv}), 8.00 (s, 1H, H-7), 8.02 (s, 1H, H-7^{v}), 7.91 (d, 1H, J = 9.2, H-4‴), 7.71 (d, 1H, J = 2.0, H-7‴), 7.68 (d, 1H, J = 3.6, H-7″), 7.65 (d, 2H, J = 8.8, H-4″ and H-4^{vi}), 7.62 (d, 1H, J = 6.4, H-7^{vi}), 7.61 (s, 1H, H-4^{v}), 7.58 (s, 1H, H-4), 7.16 (dd, 2H, J = 9.2 and 2.8, H-5‴ and H-5^{iv}), 7.15 (d, 1H, J = 2.4, H-7^{iv}), 7.09 (d, 2H, J = 8.8, H-5″ and H-5^{vi}), 4.18, 4.16, 4.14, 4.12, 4.11, 4.10, 4.08 (OCH_2CH_3); 1.58, 1.40, 1.38, 1.36, 1.35 (OCH_2CH_3); 2.05 (s, 3H, $COCH_3$); ^{13}C-NMR (DMSO-d_6, 100 MHz): δ (see Table 1); UV-Vis λ_{max} (DMSO) (log ε): 211 (4.45), 214 (4.47), 229 (4.51), 238 (4.51), 258 (4.53), 2.69 (4.65), 279 (4.57), 309 (4.54), 364 (4.58), 378 (4.56), 416 (4.62) nm; IR (KBr) ν_{max}: 3,281 (O–H), 2,980–2,933 (ArC–H), 1,657 (C═O), 1,599 (C═N), 1,556 (C═C), 1,488–1,456 (N═N), 1,263 (C–S), 1,211 (C–O), 899–519 (Ar def C═N str thiazole) cm^{-1}; ms: (ESI$^+$) m/z (%) 1,492 (9), 1,453 (9), 1,428 (17), 1,404 (17), 1,379 (15), 1,353 (18), 1,323 (16), 1,293 (11), 1,238 (17), 955 (32), 728 (69), 659 (71), 549 (72), 486 (52); anal. calcd for $C_{62}H_{63}N_{19}O_{14}S_6$: C, 49.96; H, 4.26; N, 17.85; S, 12.90. Found: C, 49.98; H, 4.28; N, 17.81; S, 12.88. Rf = 0.39.

5.4.4 2,2′-Diazene-1,2-diylbis(5-ethoxy-1,3-benzothiazole) monohydrate (4b′)

Compound **4b′** was obtained in 13% yield as a brown powder; m.p. 182–184°C (dec); ^{1}H-NMR (DMSO-d_6, 400 MHz): δ 8.01 (d, 2H, J = 9.0, H-4 and H-4′), 7.91 (m, 2H, H-7 and H-7′), 7.09 (d, 2H, J = 8.8, H-5 and H-5′), 4.13 (s, 2H, CH_2CH_3), 1.23 (s, 3H, CH_2CH_3); ^{13}C-NMR (DMSO-d_6, 100 MHz): δ 198.6 (C-2 and C-2′), 149.9 (C-6 and C-6′), 136.1 (C-3a and C-3a′), 125.2 (C-4a and C-**4a′**), 122.8 (C-4 and C-4′), 118.2 (C-5 and C-5′), 105.4 (C-7 and C-7′), 63.9 (CH_2CH_3), 14.6 (CH_2CH_3); UV-Vis: λ_{max} (DMSO) (log ε): 216 (3.90), 258 (4.01), 271 (4.22), 279 (4.10), 291 (4.04), 314 (4.19), 322 (4.21), 332 (4.16), 352 (4.19), 359 (4.19), 384 (4.03), 429 (4.01) nm; IR (KBr) ν_{max} 3,275 (N–H), 2,979–2,936 (ArC–H), 1,661 (C═N), 1,599 (C═C), 1,488–1,457 (N═N), 1,263 (C–S), 1,228 (C–O), 900–561 (Ar def C═N str thiazole) cm^{-1}; ms: (ESI$^+$) m/z (%) 599 (33), 583 (2), 569 (2), 549 (2), 535 (3), 477 (3), 410 (18), 400 (13), 380 (22), 357 (28), 343 (22), 316 (70), 201 (70); anal. calcd for $C_{18}H_{22}N_4O_{11}S_4$: C, 36.12; H, 3.70; N, 9.36; S, 21.42. Found: C, 36.09; H, 3.69; N, 9.34; S, 21.39. Rf = 0.378.

5.4.5 *N*-(4-Hydroxy-3-((6-methoxybenzo[*d*]thiazol-2-yl)diazenyl)phenyl)acetamide hexahydrate (4c)

Compound **4c** was obtained in 51% yield as brown powder; m.p. 197–199°C (dec); ^{1}H-NMR (DMSO-d_6, 400 MHz): δ 8.11 (d, 1H, J = 2.0, H-2′), 8.02 (d, 1H, J = 9.0, H-4), 7.70 (d, 1H, J = 2.4, H-7), 7.63 (dd, 1H, J = 8.8 and 2.4, H-6′), 7.18 (dd, 1H, J = 8.8 and 2.4, H-5), 7.09 (d, 1H, J = 8.8, H-5′), 3.89 (s, 3H, OCH_3), 2.04 (s, 3H, $COCH_3$); ^{13}C-NMR (DMSO-d_6, 100 MHz): δ 173.1 (CO), 168.1 (C-2), 159.1 (C-6), 153.3 (C-3a), 146.8 (C-4′), 138.4 (C-1′), 135.8 (C-3′), 132.0 (C-4a), 127.9 (C-4), 125.1 (C-6′), 118.7 (C-5′), 116.6 (C-5), 108.0 (C-2′), 105.1 (C-7), 55.8 (OCH_3), 23.8 ($COCH_3$); UV-Vis λ_{max} (DMSO) (log ε): 227 (4.06), 257 (4.12), 272 (4.26), 290 (4.09), 295 (4.08), 302 (4.12), 325 (4.19), 348 (4.18), 355 (4.19), 399 (4.23), 445 (4.25), 486 (4.22) nm; IR (KBr) $\nu_{max.}$ 3,282 (O–H and N–H), 2,941–2,834 (ArC–H), 1,658 (C═O), 1,598 (C═N), 1,555 (C═C), 1,482–1,434 (N═N), 1,264 (C–S), 1,228 (C–O), 910–510 (Ar def C═N str thiazole) cm^{-1}; ms: (ESI$^+$) m/z (%) 448 (11), 429 (11), 409 (42), 385 (10), 316 (100), 300 (22), 281 (19), 216 (70), 202 (14), 192 (21), 150 (70); anal. calcd for $C_{16}H_{26}N_4O_9S$: C, 42.66; H, 5.82; N, 12.44; S, 7.12. Found: C, 42.63; H, 5.80; N, 12.41; S, 7.10. Rf = 0.30.

5.4.6 *N*-(3-((6-Chlorobenzo[*d*]thiazol-2-yl)diazenyl)-4-hydroxyphenyl)acetamide sulfate (4d)

Compound **4d** was obtained in 61% yield as brown powder; m.p. 206–208°C (dec); ^{1}H-NMR (DMSO-d_6, 400 MHz): δ 8.20 (d, 1H, J = 2.8, H-4), 8.11 (d, 1H, J = 8.0, H-7), 7.74 (s, 1H, NH), 7.70 (m, 1H, H-8), 7.67 (m, 1H, H-6), 7.65 (s, 1H, OH), 7.55 (d, 1H, J = 8.0, H-4′), 7.51 (m, 1H, H-3′); ^{13}C-NMR (DMSO-d_6, 100 MHz): δ 198.8 (CO), 168.3 (C-2), 154.3 (C-2′), 150.5 (C-3a), 138.6 (C-4a), 135.7 (C-5′), 131.9 (C-1′), 127.0 (C-5), 126.7 (C-6), 122.1 (C-4 and C-7), 107.7 (C-4′), 105.3 (C-3′), 84.6 (C-6′), 24.0 ($COCH_3$); UV-Vis: λ_{max} (DMSO) (log ε): 216 (3.45), 233 (3.48), 267 (3.75), 287 (3.87), 297 (3.91), 309 (3.93), 343 (3.91), 373 (3.88), 390 (3.81), 402 (3.74), 504 (3.28), 529 (3.15), 557 (2.89) nm; IR (KBr) ν_{max}: 3,292 (O–H), 1,664 (C═O), 1,585 (C═N), 1,525 (C═C), 1,496–1,405 (N═N), 1,256 (C–S), 1,206 (C–O), 882–507 (Ar def C═N str thiazole) cm^{-1}; ms: (ESI$^+$) m/z (%) 442 (1), 425 (1), 409 (8), 381(1), 357 (2), 353 (4), 316 (70), 304 (10), 289 (5), 202 (30), 174 (22), 148 (41); anal. calcd for $C_{15}H_{13}ClN_4O_6S_2$: C, 40.50; H, 2.95; Cl, 7.97; N, 12.59; S, 14.41. Found: C, 40.52; H, 2.93; N, 12.58; S, 14.38. Rf = 0.73.

6 Biological assay

6.1 Antimicrobial evaluation

6.1.1 Tested microorganisms

The antimicrobial activity was performed against four bacterial and three fungal species. The selected microorganisms

were two Gram-positive *S. aureus* ATCC 25923 and *S. aureus* 18 and two Gram-negative *P. aeruginosa* PA01 and *E. coli* 64R. These microorganisms were taken from our laboratory collection. The bacterial species were grown at 37°C and maintained on a nutrient agar (NA, Conda) slant.

6.1.2 Determination of minimum inhibitory concentration (MIC) and minimum bactericidal concentration (MBC)

The antibacterial activity was performed by determining the MICs and MBCs as previously described [33]. MICs of synthesized compounds were determined by broth micro dilution. Each test sample was dissolved in dimethylsulfoxide (DMSO) to give a stock solution. This was serially diluted twofold in Mueller-Hinton broth (MHB) to obtain a concentration range of 512–0.25 µg/mL. Then, 100 µL of each sample concentration was added to respective wells (96-well micro plate) containing 90 µL of MHB and 10 µL of inoculums to give final concentration ranges of 256 to 0.125 µg/mL. The final concentration of microbial suspensions was 10^6 CFU/mL for bacteria. Dilution of ciprofloxacin (Sigma-Aldrich, Steinheim, Germany) was used as a positive control. Broth with 10 µL of DMSO was used as a negative control. The MIC values of samples were determined by adding 50 µL of a 0.2 mg/mL *p*-iodonitrotetrazolium violet solution followed by incubation at 37°C for 30 min. Viable microorganisms reduced the yellow dye to pink color. MIC values were defined as the lowest sample concentrations that prevented this change in color, indicating a complete inhibition of bacterial growth [33]. For the determination of MMC values, a portion of liquid (5 µL) from each well that showed no growth of microorganism was plated on Mueller-Hinton agar and incubated at 37°C for 24 h. The lowest concentrations that yielded no growth after this subculturing were taken as the MBC values [33]. All the tests were performed in triplicate.

Acknowledgments: J.T. is grateful to Gilbert Kirsch and Véronique Vaillant for running the NMR spectra.

Funding information: The authors state no funding involved.

Conflict of interest: The authors state no conflict of interest.

Data availability statement: The datasets generated during and/or analyzed during the current study are available from the corresponding author on reasonable request.

References

[1] Abbott FV, Fraser MI. Use and abuse of over-the-counter analgesic agents. J Psychiatry Neurosci. 1998;23(ll):13–34.
[2] Straube A, Aicher B, Fiebich BL, Haag G. Combined analgesics in (headache) pain therapy: shotgun approach or precise multi-target therapeutics? BMC Neurol. 2011;11(43):1–15.
[3] Anderson BJ. Paracetamol (Acetaminophen): mechanisms of action. Paediatr Anaesth. 2008;18:915–21.
[4] Amornyotin S. Sedative and analgesic drugs for gastrointestinal endoscopic procedure. J Gastroenterol Hepatol Res. 2014;3(7):1133–44.
[5] Sinha M, Gautam L, Shukla PK, Kaur P, Sharma S, Singh TP. Current perspectives in NSAID-induced gastropathy. Mediators Inflamm. 2013;2013:258209. 11 pages.
[6] Bannwarth B. Gastrointestinal safety of paracetamol: is there any cause for concern? Opin Drug Saf. 2004;3(4):269–72.
[7] Yoon E, Babar A, Choudhary M, Kutner M, Pyrsopoulos N. Acetaminophen-induced hepatotoxicity: a comprehensive update. J Clin Transl Hepatol. 2016;4:131–42.
[8] Fontana RJ. Acute liver failure including acetaminophen overdose. Med Clin N Am. 2008;92:761–94.
[9] Ugwu DI, Okoro UC, Ukoha PO, Gupta A, Okafor SN. Novel anti-inflammatory and analgesic agents: synthesis, molecular docking and *in vivo* studies. J Enzyme Inhib Med Chem. 2018;33(1):405–15.
[10] Kamal A, Syed MAH, Mohammed SM. Therapeutic potential of benzothiazoles: a patent review (2010–2014). Expert Opin Ther Pat. 2014;25(3):1–15.
[11] Sharma PC, Sinhmar A, Sharma A, Rajak H, Pathak DP. Medicinal significance of benzothiazole scaffold: an insight view. J Enzyme Inhib Med Chem. 2013;28(2):240–66.
[12] Gaffer HE, Fouda MMG, Khalifa ME. Synthesis of some novel 2-amino-5-arylazothiazole disperse dyes for dyeing polyester fabrics and their antimicrobial activity. Molecules. 2016;21:122–31.
[13] Beuchet P, Varache-Lembège M, Neveu A, Léger JM, Vercauteren J, Larrouture S, et al. New 2-sulfonamidothiazoles substituted at C-4: synthesis of polyoxygenated aryl derivatives and in vitro evaluation of antifungal activity. Eur J Med Chem. 1999;34:773–9.
[14] Kakade KP. Complex of 2-Amino acetate-6-fluoro benzothiazole with some metal ion, its effect on germination of wheat plant. J Chem Pharm Res. 2013;5(2):299–304.
[15] Gong Z, Peng Y, Qiu J, Cao A, Wang G, Peng Z. Synthesis, *in vitro*-glucosidase inhibitory activity and molecular docking studies of novel benzothiazole-triazole derivatives. Molecules. 2017;22(1):1555.
[16] Djeukoua DKS, Sopbue FE, Tamokou J-D-D, Tsemeugne J, Simon PFW, Tsopmo A, et al. Synthesis, characterization, antimicrobial activities and electrochemical behavior of new phenolic azo dyes from two thienocoumarin amines. Arkivoc. 2019;Part VI:416–30.
[17] Tamokou J-D-D, Tsemeugne J, Sopbué FE, Sarkar P, Kuiate J-R, Djintchui AN, et al. Antibacterial and cytotoxic activities and SAR of some azo compounds containing thiophene backbone. Pharmacologia. 2016;7(4):182–92.
[18] Sopbué FE, Tsemeugne J, Tamokou J-D-D, Djintchui AN, Kuiaté J-R, Sondengam BL. Synthesis and antimicrobial

activities of some novel thiophene containing azo compounds. Heterocycl Commun. 2013;19:253–9.
[19] Tsemeugne J, Sopbué FE, Tamokou J-D-D, Tonle I, Kengne CI, Djintchui NA, et al. Electrochemical behavior and *in-vitro* antimicrobial screening of some thienylazoaryls dyes. Chem Cent J. 2017;11(11):119.
[20] Tsemeugne J, Sopbué FE, Tamokou J-D-D, Rohand T, Djintchui AN, Kuiate J-R, et al. Synthesis, characterization, and antimicrobial activity of a novel trisazo dye from 3-amino-4H-thieno[3,4-c][1]benzopyran-4-one. Int J Med Chem. 2018;2018:9197821. 8 pages.
[21] Rufchahi EOM, Yousefi H, Mohammadinia M. Synthesis and spectral properties of some azo disperse dyes containing a benzothiazole moiety. J Mol Liq. 2013;188:173–7.
[22] Maliyappa MR, Keshavayya J, Mahanthappa M, Shivaraj Y, Basavarajappa KV. 6-Substituted benzothiazole base dispersed azo dyes having pyrazole moiety: Synthesis, characterization, electrochemical and DFT studies. J Mol Struct. 2020;1199:126959.
[23] Tupys A, Kalembkiewicz J, Ostapiuk Y, Matiichuk V, Tymoshuk O, Nicka EW, et al. Synthesis, structural characterization and thermal studies of a novel reagent 1-[(5-benzyl-1,3-thiazol-2-yl)diazenyl]naphthalene-2-ol. J Therm Anal Calorim. 2017;127:2233–42.
[24] Kirk W, Johnson JR, Blomquist AT. Spectroscopic studies of keto–enol tautomeric equilibrium of azo dyes. Org Chem. 1943;3:557.
[25] Bhargava PN, Baliga BT. Studies on 2-aminobenzothiazoles. J Indian Chem Soc. 1958;35:807–10.
[26] Zhao C, Han Y-Z, Dai S, Chen X, Yan J, Zhang W, et al. Microporous cyclic titanium-oxo clusters with labile surface ligands. Angew Chem Int Ed. 2017;56(51):16252–6.
[27] Eslava S, Papageorgiou AC, Beaumont SK, Kyriakou G, Wright DS, Lambert RM. Synthesis, characterization, and surface tethering of sulfide-functionalized Ti16-oxo-alkoxy cages. Chem Mater. 2010;22(18):5174–8.
[28] Doyle MP, Dellaria JF, Siegfried B Jr, Bishop SW. Reductive deamination of arylamines by alkyl nitrites in *N*,*N*-dimethylformamide. A direct conversion of arylamines to aromatic hydrocarbons. J Org Chem. 1977;42(34):3494–8.
[29] Kornblum N. Organic Reactions. New York: John Wiley and Sons Inc; 1944.
[30] Huang J, Ren H, Zhang R, Lidong W, Zhai Y, Meng Q, et al. Supramolecular self-assembly of perylene bisimide based rigid giant tetrahedra. ACS Nano. 2020;14(7):8266–75. doi: 10.1021/acsnano.0c01971.
[31] Haydon DJ, Benett JM, Brown D, Collins D, Galbraith G, Lancett P, et al. Creating an antibacterial with *in vivo* efficacy: synthesis and characterization of potent inhibitors of the bacterial cell division protein FtsZ with improved pharmaceutical properties. J Med Chem. 2010;53:3927–36.
[32] Gjorgjieva M, Tomašič T, Kikelj D, Mašič LP. Benzothiazole-based compounds in antibacterial drug discovery. Curr Med Chem. 2018;25:1–19.
[33] Nyaa TBL, Tapondjou AL, Barboni L, Tamokou J-D-D, Kuiate J-R, Tane P, et al. NMR assignment and antimicrobial/antioxidant activities of 1-hydroxyeuscaphic acid from the seeds of Butyrospermum parkii. Nat Prod Sci. 2009;15:76–82.